High lying $E0$ strength in ^{12}C

D. H. Youngblood, Y.-W. Lui, and H. L. Clark
Cyclotron Institute, Texas A&M University, College Station, Texas 77843
(Received 25 November 1997)

The excitation region in ^{12}C from 7 MeV$<E_x<$60 MeV was studied with inelastic scattering of 240-MeV α particles at small angles including 0° where $E0$ strength is enhanced. The strengths of known 0^+ states at $E_x=7.655$ MeV and $E_x=10.3$ MeV were obtained and $E0$ strength was observed to be distributed between $E_x=14$ MeV and $E_x=30$ MeV with a centroid of 21.5 ± 0.4 MeV and an rms width of 3.1 ± 0.2 MeV containing $14.5\pm4.0\%$ of the isoscalar $E0$ energy-weighted sum rule. Angular distributions and strengths of the $E_x=4.439$ MeV 2^+, 9.641 MeV 3^-, and 10.844 MeV 1^- states were also obtained. [S0556-2813(98)05704-5]

PACS number(s): 24.30.Cz, 25.55.Ci, 27.20.+n

Giant resonances (GR's) are usually thought of as strongly collective modes present primarily in heavier nuclei. Generally experiments on lighter nuclei such as ^{12}C have identified little or no GR strength. $E1$ strength corresponding to about 19–29 % of the TRK sum rule has been located [1] and $E2$ strength corresponding to about 16% of the isoscalar $E2$ strength has been located in ^{12}C [2]. There have been no reports of small-angle experiments looking for high-lying $E0$ strength in ^{12}C. We have studied the GR region of ^{12}C with the inelastic scattering of 240 MeV α particles at and near 0° where monopole strength is enhanced and competing particle pickup breakup peaks are well outside the region of interest and used the spectrum subtraction technique [3–5] on small-angle ^{12}C(α,α') data to identify high-lying $E0$ strength.

The experimental technique has been described thoroughly in Refs. [4] and [5] and is summarized below. A beam of 240 MeV α particles from the Texas A&M K500 superconducting cyclotron bombarded a self-supporting natural C foil 2.0 mg/cm^2 thick located in the target chamber of the multipole-dipole-multipole spectrometer [6]. The beam was delivered to the spectrometer through a beam analysis system having two bends of 88° and 87° [7]. The beam was limited by slits after the first bend, and the second bend was used for clean up, with slits located so as not to intercept the primary beam. The horizontal acceptance of the spectrometer was 4° and ray tracing was used to reconstruct the scattering angle. The vertical acceptance was set at $\pm2°$. When the spectrometer central angle ($\theta_{\rm spec}$) was set to 0°, the beam passed beside the detector and was stopped in a carbon block behind the detector. At $\theta_{\rm spec}=0°$, runs with an empty target frame showed α particles uniformly distributed in position at a rate about 1/2000 of that with a target in place.

The focal plane detector covered approximately 55 MeV of excitation from 7 MeV$<E_x<$62 MeV and measured position and the angle in the scattering plane. The out-of-plane scattering angle ϕ was not measured. Position resolution of approximately 0.9 mm and scattering angle resolution of about 0.09° were obtained. Giant-resonance data were taken for ^{12}C with $\theta_{\rm spec}$ set at 0°, covering the angular range from $-2°$ to $+2°$.

Data were also taken with ^{12}C, ^{24}Mg, and ^{28}Si targets at $\theta_{\rm spec}=3.5°$ at the actual field settings used in the experiments to obtain an energy calibration. The positions of the 9.641 and 18.350 MeV states [8] in ^{12}C, the 10.18, 18.67, and 20.43 MeV states [9,10] in ^{28}Si and the 12.86 and 17.36 MeV states [10] in ^{24}Mg were used to obtain momentum calibrations linear in position for each of the spectra. The energies of these known narrow peaks between 9 and 21 MeV were consistently reproduced better than 50 keV. Data were taken for ^{12}C at a field setting where the elastic scattering was on the detector in order to obtain cross sections for the $E_x=4.439$ MeV and 7.655 MeV states.

Each data set was divided into ten angle bins, each corresponding to $\Delta\theta\simeq0.4°$ using the angle obtained from ray tracing. ϕ is not measured by the detector, so the average angle for each bin was obtained by integrating over the height of the solid angle defining slit and the width of the angle bin. Cross sections were obtained from the charge collected, target thickness, dead time and known solid angle. The cumulative uncertainties in target thickness, solid angle, etc. result in about a $\pm10\%$ uncertainty in absolute cross sections.

Spectra obtained for ^{12}C with the spectrometer at 0° for several angle gates are shown in Fig. 1. At the smallest angle, corresponding to an average laboratory angle of $\theta_{\rm avg}=1.1°$, the well-known $E_x=7.655$ MeV and 10.3 MeV $L=0$ states are prominent and the $E_x=9.641$ MeV $L=3$ state is weak. At larger angles the $L=0$ states are progressively weaker and the $L=3$ state stronger. Also the 10.844 MeV $L=1$ state shows prominently at 2.7°. The low excitation cutoff in the detector was around $E_x=7$ MeV, but the effective solid angle varies rapidly with scattering angle below $E_x=8$ MeV so the strength of the 7.655 MeV peak in the spectra is not a reliable measure of its cross section relative to the rest of the spectrum. Angular distributions were obtained for the 4.439, 7.655, 9.641, 10.3, and 10.844 MeV states and are shown in Fig. 2. Since monopole strength is strongly forward peaked while higher multipoles are nearly flat at small angles [4,5] a ''spectrum of $E0$ strength'' was generated [3–5] by subtracting the spectrum taken at center-of-mass angle 2.7° from the spectrum taken at 1.4°. This is shown in Fig. 3(a). The isovector giant dipole resonance (GDR) is also forward peaked (excited only by Coulomb excitation in ^{12}C), but is much weaker than the other multipolarities and has no impact on this analysis.

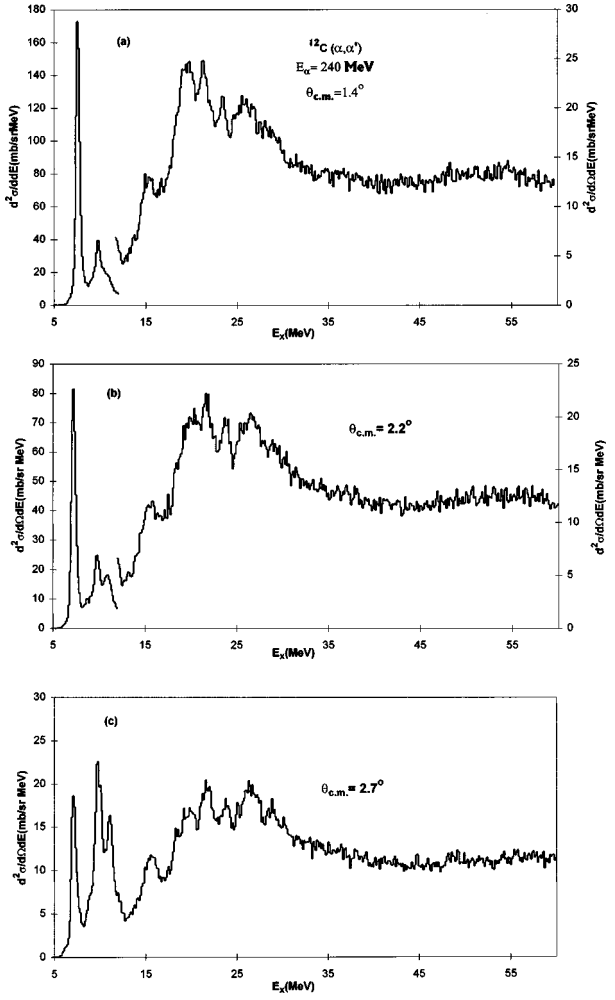

FIG. 1. Spectra obtained for $^{12}\mathrm{C}(\alpha,\alpha')$ at $E_\alpha = 240$ MeV for three angles. The average center-of-mass angles are indicated. The double differential cross section up to about 12 MeV is given by the left scale and that above 12 MeV is given by the right scale for the 1.4° and 2.2° spectra. The left scale applies to the entire 2.7° spectrum.

The transition densities and sum rules for various multipolarities are described thoroughly by Satchler [11]. For the $E0$ strength we have used the transition density corresponding to a breathing-mode oscillation:

$$U = -\alpha_0[3\rho + r d\rho/dr],$$

where for a state that exhausts the energy-weighted sum rule (EWSR):

$$\alpha_0{}^2 = 2\pi(\hbar^2/m)(A\langle r^2\rangle E_x)^{-1}.$$

Calculations for the 10.844 MeV $L=1$ state were carried out with an isoscalar dipole form factor [4,12]. The form factors used for other multipoles in this work are given in Ref. [4].

Distorted-wave Born approximation (DWBA) and optical-model calculations were carried out with the code PTOLEMY [13]. Input parameters for PTOLEMY were modified

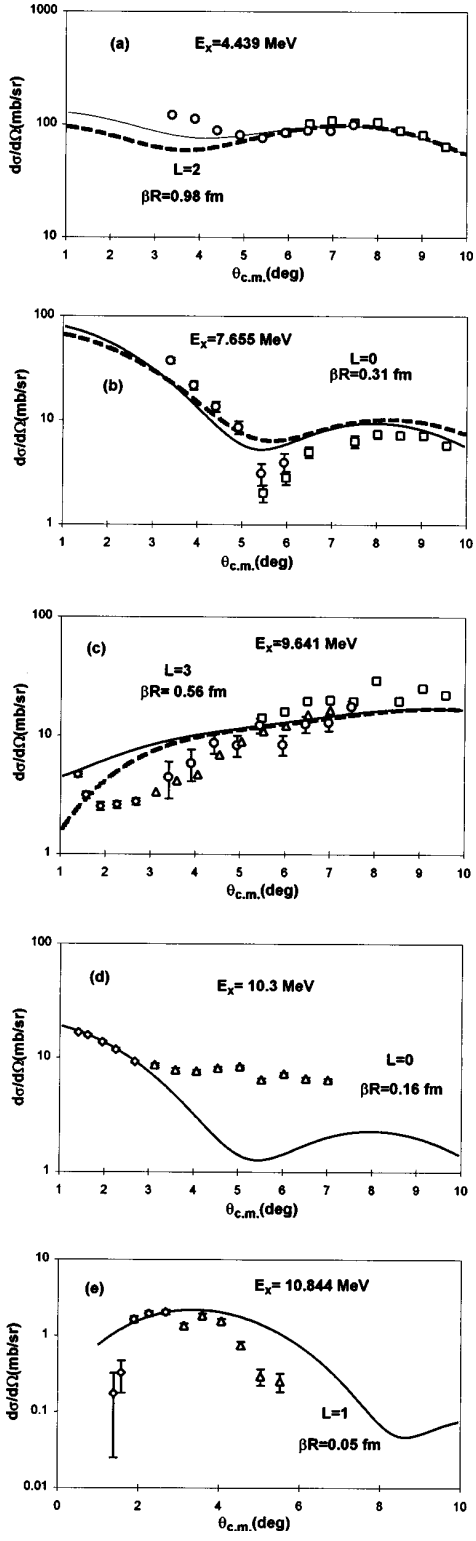

FIG. 2. Angular distributions of the differential cross section for inelastic α scattering to five states ^{12}C plotted versus average center-of-mass angle. The excitation energy for each state [8] is given. The lines show DWBA calculations for the L transfer and βR given. The solid line represents calculations using ^{28}Si parameters from Ref. [5] and the dashed line represents calculations using ^{12}C parameters from Ref. [16]. The square data points were taken with the elastic data at $\theta_{\mathrm{spec}} = 5.5°$ and the circles were taken with elastic data at $\theta_{\mathrm{spec}} = 3.5°$. The diamonds and triangles were taken with the giant resonance data at $\theta_{\mathrm{spec}} = 0°$ and 3.5°, respectively. When not shown, statistical errors are smaller than the data points.

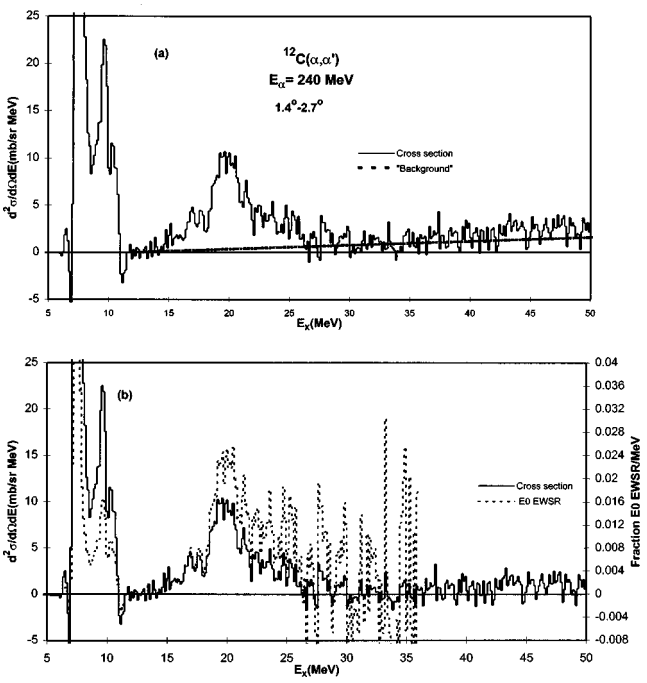

FIG. 3. (a) The solid line shows the double differential cross section adjusted to 0° of the difference spectrum obtained by subtracting the spectrum taken at 2.7° from the spectrum at 1.4°. (b) The solid line shows the double differential cross section after subtraction of the background from the spectrum in (a). The gray line shows fraction of the isoscalar $E0$ EWSR obtained by dividing the cross section by the cross section expected for 100% of the $E0$ EWSR.

[14] to obtain a relativistic kinematically correct calculation. The amplitudes of the transition densities for the various multipoles obtained from the expressions in Ref. [4] for 100% of the respective sum rules are given in Table I. Radial moments for ^{12}C were obtained by numerical integration of the Fermi-mass distribution assuming $c=2.321$ fm and $a=0.568$ [15].

Since optical-model parameters are not available for 240 MeV α particles on ^{12}C, the optical-model parameters obtained for ^{28}Si [5] were used. Calculations for discrete states were also carried out with parameters obtained for 166 MeV α on ^{12}C by Tatischeff and Brissaurd [16]. Calculations with both optical-model sets are shown superimposed on the data for the discrete states in Fig. 3. Values of βR used for the $E_x=4.439$ and 9.641 MeV states are those obtained by Tatischeff and Brissaurd [16] and can be seen to fit the data moderately well for both sets of optical parameters. They did not report β values for the 7.655 or 10.3 MeV states. The calculations for the 4.439 MeV $L=2$ state fit the data well for angles above 5°, but neither predicts the increase in cross section below 5°. The calculations agree well with the data at smaller angles for the 7.655 0^+ state but the calculation is much higher than the data at the second maximum. Data for the 7.655 MeV state taken with the magnet set for the GR data are very near the detector cutoff (due to rays being intercepted by portions of the detector) and cross sections are not reliable, hence data for this state near 0° are not available. The data for the 10.3 MeV 0^+ state are fit well by the calculation at small angles where the state is strong, but are well above the calculation in the minimum, probably because of difficulties in separating this broad state from the other unresolved states at 11.6, 11.83, and 12.71 MeV in the presence of the very strong 9.641 MeV state. The data for the 10.844 MeV 1^- state fall off more sharply than the calculation on both sides of the maximum, probably due to difficulties in separating this peak from the much broader 10.3 MeV state.

TABLE I. Excitation energies, βR values, and $E0$ strength obtained for ^{12}C states. The energy of the 7.655 MeV state was not obtained in this work (see text).

E_x (MeV)	J^π	βR (fm)	% $E0$ EWSR %	Γ (MeV)
7.655	0^+	0.31	5.0	
9.65±0.03	3^-	0.56		
10.18±0.07	0^+	0.16	1.8	2.14±0.15
10.96±0.10	1^-	0.05		

TABLE II. Parameters obtained for $E0$ strength between $E_x=14-30$ MeV in ^{12}C. Errors are statistical only. Systematic errors due to angle calibration discussed in text are shown in parentheses.

	Background subtracted	No Subtraction
% $E0$ EWSR	14.5±1.3(4.0)	18.9±1.3(4.0)
Energy-m_1/m_0 (MeV)	21.5±0.4	22.6±0.3
rms width (MeV)	3.1±0.2	2.8±0.2

If all of the cross section in the difference spectrum [Fig. 3(a)] is assumed to be $E0$, the total $E0$ strength can then be obtained. From this the 10.3 MeV state was found to exhaust 1.9±0.1% of the $E0$ EWSR in agreement with the 1.8% found with the fit shown in Fig. 2(d). $E0$ strengths obtained for the 7.655 and 10.3 MeV states are given in Table I. For these states the fraction of the $E0$ EWSR they represent, assuming a breathing-mode transition density, is given in addition to the βR. Also given in Table I are the energies and βR values obtained for the higher states. The width obtained for the $E_x=10.3$ MeV state is also given. The energies of the 7.655 and 4.439 MeV states were not extracted because they were observed only in the elastic-scattering runs and energy calibrations were not obtained for these runs. All of the energies and the width for the 10.3 MeV states are in excellent agreement with accepted values [8].

The $E0$ strengths in the continuum between $E_x=14-30$ MeV are summarized in Table II. The strength in the difference spectrum between $E_x=14-30$ MeV corresponds to 18.9±1.3% of the $E0$ EWSR. In a previous work [5] we have shown that the $E0$ strength obtained from difference spectra agree with that obtained by fitting angular distributions. However, in that work [5] we also concluded that some of the apparent $E0$ strength in the continuum may be due to other (unidentified) reaction mechanisms which are also forward peaked. In an attempt to remove the contribution of these other mechanisms, a linear ''background'' was subtracted from the ''subtracted spectrum'' as illustrated in

Fig. 2(b). The background was assumed to be zero around $E_x = 12$ MeV where the subtracted spectrum is zero, and the line was drawn to the average background at $E_x = 35$ MeV, the upper extent of the GR peak in ^{28}Si. The parameters obtained for $E0$ strength above $E_x = 14$ MeV in ^{12}C with and without the background subtraction are given in Table I. With this subtraction the remaining strength between $E_x = 14-30$ MeV corresponds to $14.5 \pm 1.3\%$ of the $E0$ EWSR.

This work was supported in part by the Department of Energy under Grant No. DE-FG03-93ER40773 and by The Robert A. Welch Foundation.

[1] B. L. Berman, Lawrence Livermore Laboratory Report, UCRL-78482 (1976).
[2] H. Riedesel, K. T. Knopfle, H. Breuer, P. Doll, G. Mairle, and G. J. Wagner, Phys. Rev. Lett. **41**, 377 (1978).
[3] S. Brandenburg, R. De Leo, A. G. Drentje, M. N. Harakeh, H. Sakai, and A. van der Woude, Phys. Lett. **130B**, 9 (1983).
[4] D. H. Youngblood, Y.-W. Lui, and H. L. Clark, Phys. Rev. C **55**, 2811 (1997).
[5] D. H. Youngblood, H. L. Clark, and Y.-W. Lui, Phys. Rev. C **57**, 1134 (1998).
[6] D. M. Pringle, W. N. Catford, J. S. Winfield, D. G. Lewis, N. A. Jelley, K. W. Allen, and J. H. Coupland, Nucl. Instrum. Methods Phys. Res. A **245**, 230 (1986).
[7] D. H. Youngblood and J. D. Bronson, Nucl. Instrum. Methods Phys. Res. A **361**, 37 (1995).
[8] F. Ajzenberg-Selove, Nucl. Phys. **A506**, 1 (1990).
[9] K. van der Borg, M. N. Harakeh, and A. van der Woude, Nucl. Phys. **A365**, 243 (1981).
[10] Y.-W. Lui, J. D. Bronson, D. H. Youngblood, and Y. Toba, Phys. Rev. C **31**, 1641 (1985).
[11] G. R. Satchler, Nucl. Phys. **A472**, 215 (1987).
[12] M. N. Harakeh and A. E. L. Dieperink, Phys. Rev. C **23**, 2329 (1981).
[13] M. Rhoades-Brown, M. H. Macfarlane, and S. C. Pieper, Phys. Rev. C **21**, 2417 (1980); M. H. Macfarlane and S. C. Pieper, Argonne National Laboratory Report No. ANL-76-11, Rev. 1, 1978 (unpublished).
[14] G. R. Satchler, Nucl. Phys. **A540**, 533 (1992).
[15] G. Fricke, C. Bernhardt, K. Heilig, L. A. Schaller, L. Schellenberg, E. B. Shera, and C. W. DeJager, At. Data Nucl. Data Tables **60**, 177 (1995).
[16] B. Tatischeff and I. Brissaud, Nucl. Phys. **A155**, 89 (1970).